Deformed-helix ferroelectric liquid-crystal spatial light modulator that demonstrates high diffraction efficiency and 370-line pairs/mm resolution

David V. Wick, Ty Martinez, Michael V. Wood, James M. Wilkes, Mark T. Gruneisen, Vladimir A. Berenberg, Michael V. Vasil'ev, Arkady P. Onokhov, and Leonid A. Beresnev

New liquid-crystal media and photoconductor materials are being utilized in spatial light modulators to increase their resolution, diffraction efficiency, speed, and sensitivity. A prototypical device developed for real-time holography applications has shown an 8% diffraction efficiency from a holographic grating with a spatial frequency of 370 line pairs/mm (lp/mm). At 18 lp/mm the device has demonstrated a 31% diffraction efficiency with a 600-μs hologram write time using 400-nJ/cm^2 write beams. © 1999 Optical Society of America

OCIS codes: 090.1000, 230.6120, 160.2260, 160.3710.

1. Introduction

Dynamic compensation of severe aberrations by holographic phase subtraction requires real-time holographic (RTH) recording media that are capable of simultaneous high diffraction efficiencies (DE's), fast response times, high resolution, and high sensitivity. Optically addressed spatial light modulators (OASLM's) previously were used to compensate hundreds of waves of aberration caused by poor-quality primary mirrors in telescopic systems with write-beam intensities as low as 50 μW/cm^2 but with limited DE, speed, and resolution.[1–3]

A schematic diagram of a typical OASLM used for RTH phase subtraction is shown in Fig. 1. The device consists of a photoconductor (PC) and a thin liquid-crystal (LC) layer situated between a pair of transparent electrodes. If the device is used in a reflective geometry there may also be a high-reflectivity mirror between the PC and the LC. A diffraction hologram is written in the device by means of interfering two mutually coherent wave fronts on the PC. The resulting interference pattern modifies the local conductivity of the PC, creating a spatially varying electric field across the LC layer. The local field then induces a reorientation of the LC molecules, creating a spatial pattern in the LC layer that corresponds directly to the interference pattern on the PC.[4] This distribution of molecules creates a phase or polarization grating that diffracts the read beam. In the case of aberration compensation an aberrated image-bearing beam is diffracted from a grating that contains the aberration information, thus subtracting out the aberrations and yielding a corrected image.[5]

Historically, the performance of OASLM's has been limited by both the PC and the LC media. To achieve DEs greater than 1%, it was necessary for devices that used an amorphous hydrogenated silicon (a-Si:H) PC to be limited to spatial frequencies of less than 110 line pairs/mm[6–8] (lp/mm). Organic-polymer PC's were used to increase the resolution, but the response time of the device suffers because of low carrier mobility.[9] Historically, among LC media there has been a trade-off between the refresh rate (i.e., the rate at which the grating can repeatedly be written, read, and erased) and high DE. Nematic LC devices were developed with DE's in excess of 30%, approaching the theoretical limits for an analog

D. V. Wick (wickd@plk.af.mil), T. Martinez, M. V. Wood, J. M. Wilkes, and M. T. Gruneisen are with the U.S. Air Force Research Laboratory, AFRL/DEBS, 3550 Aberdeen Avenue Southeast, Kirtland Air Force Base, New Mexico 87117. V. A. Berenberg, M. V. Vasil'ev, and A. P. Onokhov are with the Institute for Laser Physics, SC Vavilov State Optical Institute, St. Petersburg 199034, Russia. L. A. Berenesev is with the U.S. Army Research Laboratory, Intelligent Optics Laboratory, 2800 Powder Mill Road, Adelphi, Maryland 20783.

Received 18 September 1998; revised manuscript received 12 February 1999.

0003-6935/99/173798-06$15.00/0

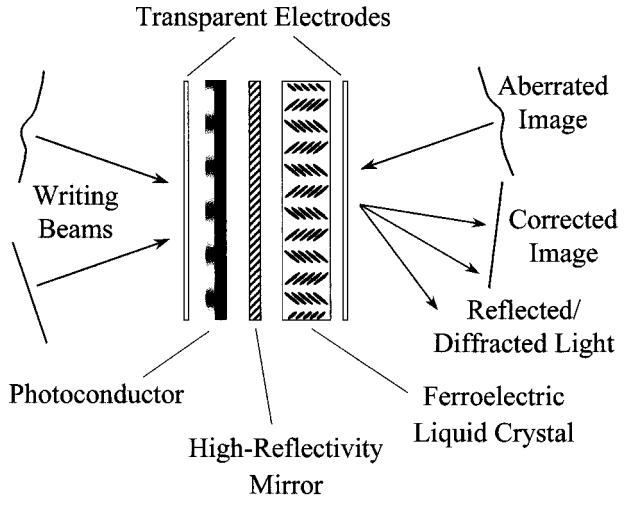

Fig. 1. OASLM showing write, aberrated-read, and reflected/diffracted beams. Note that the DHFLC molecules actually rotate within the plane that is parallel to the LC layer (normal to the page).

device.[10] Unfortunately, typical refresh rates for these devices are limited to approximately 30 Hz because of the slow recovery times of the LC media, and diffraction occurs for only one linear-polarization state. On the other hand, surface-stabilized ferroelectric LC devices can operate with refresh rates greater than 1 kHz, but the low-tilt-angle LC media that previously were available restrict the DE to less than 10%.[11]

Recently, OASLM's that use a deformed-helix ferroelectric LC (DHFLC) have received considerable attention as a result of their potential for gray-scale response.[12] Although such devices have been described in the literature,[7,8] the relatively low tilt angles (27° and 23°) of these DHFLC devices are far from the ideal of 45° that is required for optimum DE.[2]

OASLM's that utilize a high-tilt-angle DHFLC and a carbon-doped a-Si:H (a-Si_{1-x}:C_x:H) PC are currently being developed to achieve high DE and a fast response time simultaneously with minimal write-light irradiance at high resolution. DHFLC media are available with molecular tilt angles that approach 45° and can be used to generate DE's that approach theoretical limits.[2] The a-Si:H can be doped with carbon to reduce the dark conductivity, which allows for higher resolution while still maintaining relatively fast response times.[9,13] Here we describe characterization measurements performed on a prototypical DHFLC device that uses an a-Si_{1-x}:C_x:H photoconductor. This OASLM was built for the U.S. Air Force by the Institute for Laser Physics in St. Petersburg, Russia.

2. Experiment

High resolution and high photosensitivity were obtained simultaneously in the above-described OASLM by experimental variation of the amount of carbon in the PC layer. The a-Si_{1-x}:C_x:H layer was deposited by plasma-enhanced chemical-vapor deposition in a multichamber setup.[14] During this procedure the carbon concentration was varied by means of adjusting the flows of CH_4 and SiH_4 gaseous mixtures. The thickness of the PC is approximately 1.2 μm, and the carbon content is given by $x = 0.33$.

The response time and the DE of this OASLM is determined primarily by the reorientation of the ferroelectric molecules with changing electric fields. The short-pitch, high-polarization mixture used in this device was developed specifically for RTH applications and resulted from further improvements to previous mixtures.[9] In this device the LC molecules are aligned in the planar, or homogenous, orientation through a technique that is described in detail elsewhere.[15] The LC medium exhibits a smectic C* phase between 0 °C and 61 °C. At 23 °C the strongly twisted helical structure has a pitch of 0.18 μm, a molecular tilt angle of 39.5°, and a spontaneous polarization of 115 nC/cm^2. The nominal thickness of the LC layer is 12 μm.

In contrast to more conventional surface-stabilized ferroelectric LC's, the DHFLC molecules maintain their normal helical arrangement in an unbiased state. Because the pitch of this helix is less than an optical wavelength, incident light will experience an index of refraction that is spatially averaged over the helical arrangement of molecules. This averaging can be described by an averaged-index ellipsoid whose spatial characteristics and temporal dynamics determine the DE and the speed of the OASLM.[16] A low applied voltage of the order of several volts will distort the helix and cause a transverse rotation of the spatially averaged-index ellipsoid. If the electric field across the LC layer is high enough the helix is believed to untwist completely, leading to maximum index ellipsoid rotation.

The temporal response of this averaged-index ellipsoid to varying electric fields was investigated using the experimental setup shown in Fig. 2(a). A cw linearly polarized collimated beam at 810 nm is incident normal to the surface of the OASLM. An alternating positive–negative polarity square-wave voltage is applied across the device to rotate the index ellipsoid. The OASLM is rotated about its surface normal until either the major or the minor axis of the index ellipsoid is aligned with the input polarization wave when the device has a large negative bias. The transmitted wave passes through an orthogonal analyzer before it is measured by a fast photodiode. Figure 2(b) shows the transmission through the analyzer (solid curve) as the voltage across the OASLM (dashed curve) is switched from +42 V to −42 V. When the voltage is switched the index ellipsoid rotates through twice the molecular tilt angle, or approximately 80°. The thickness of the DHFLC layer is approximately 13 μm, and the net optical retardance at 810 nm is approximately λ/2, leading to a 160° polarization rotation in the input wave. Thus the transmission through the analyzer is nonzero initially, when the device is positively biased, and eventually goes to zero after the voltage is switched. As

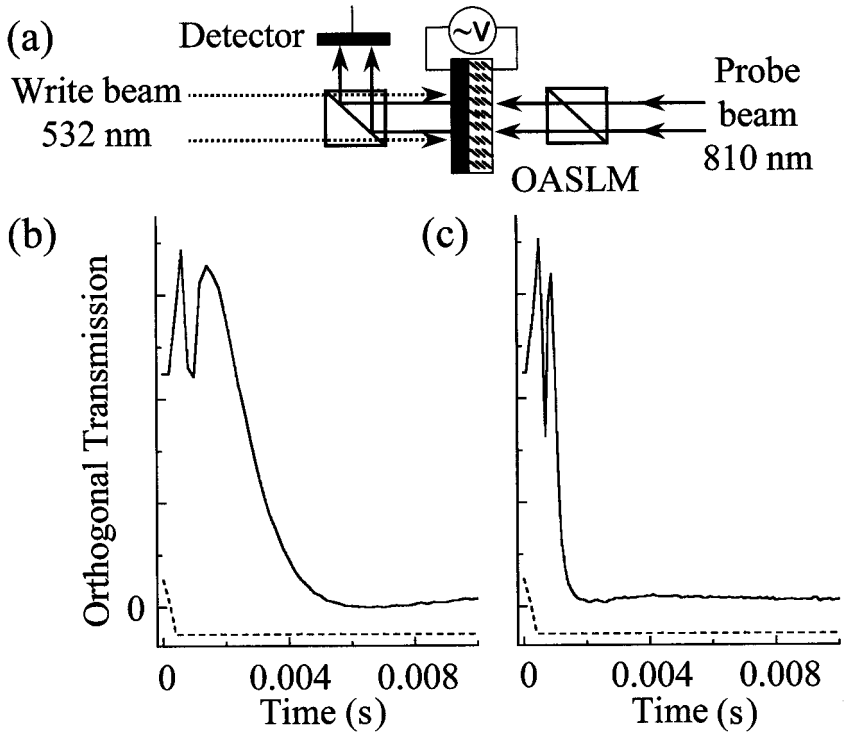

Fig. 2. (a) Experimental configuration for measuring molecular-switching dynamics. The graphs show the measured switching dynamics (b) without and (c) with PC illumination. The dashed curve shows the bias voltage.

the molecules reorient themselves after the voltage is switched, a peak occurs in the transmission when the averaged-index ellipsoid passes through 45°. The oscillatory behavior during this reorientation is currently being investigated, but we believe that it is primarily due to scattering that occurs in the LC layer when the polarity of the voltage across the OASLM is switched. Figure 2(b) shows that it takes approximately 5 ms for the index ellipsoid to reach the steady state for this voltage.

The molecular-switching time can be reduced dramatically by illumination of the PC with a spatially uniform write beam. Photoinduced carriers increase the conductance of the PC layer; as a result, the internal field across the LC layer is enhanced, which can significantly increase the speed at which the index ellipsoid rotates. Figure 2(c) shows the transmission when a single write pulse of 275 nJ/cm^2 at 532 nm illuminates the PC layer while the voltage is switched from +42 V to −42 V. The rotation time for the index ellipsoid under these conditions is reduced to slightly more than 1 ms. This switching time can be reduced further by an increase in either the write-pulse energy or the bias voltage.

The difference in molecular-switching times with and without PC illumination can be used to write a transient diffraction hologram in the OASLM. Figure 3 shows schematically how the writing of the transient holographic grating takes place. Initially, the LC molecules are all aligned by a high negative voltage applied across the OASLM. All the LC molecules within the DHFLC layer are oriented at −40°, and there is no diffraction. The voltage is switched to a lower positive voltage, and the write pulses are introduced, creating an interference pattern with intensity modulation in one dimension on the PC. Photoexcited carriers are created within only the bright areas of this fringe pattern. The applied voltage causes these carriers to migrate across the PC layer, increasing the local electric field across the LC layer. Thus the interference pattern on the PC induces a spatially varying field across the LC layer.

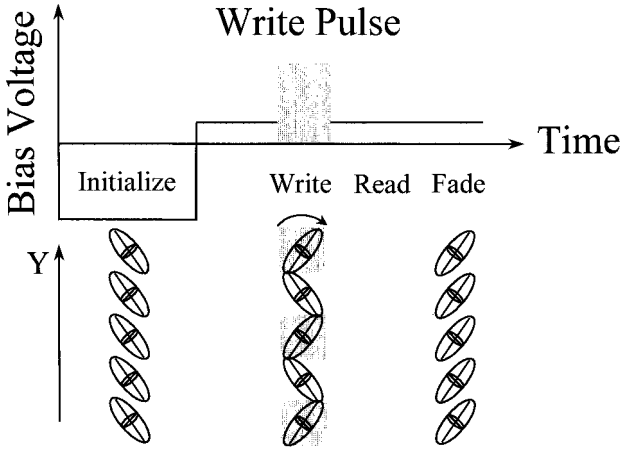

Fig. 3. Timing diagram for transient hologram formation and decay. Shown are the OASLM's bias voltage, the spatially and temporally modulated write pulse, and the orientation of the averaged-index ellipsoid.

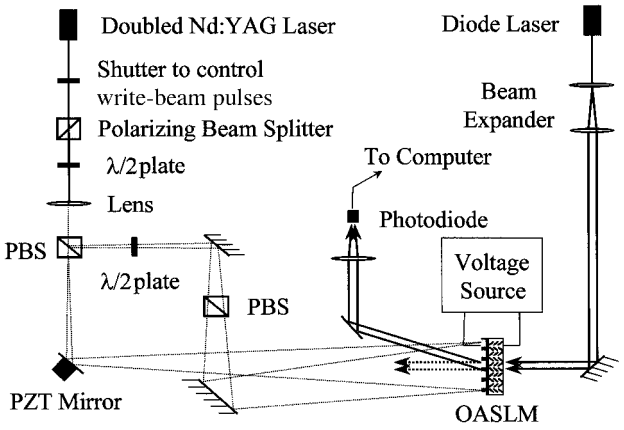

Fig. 4. Experimental setup for measuring the DE. PZT, piezoelectric transducer; PBS, polarizing beam splitter.

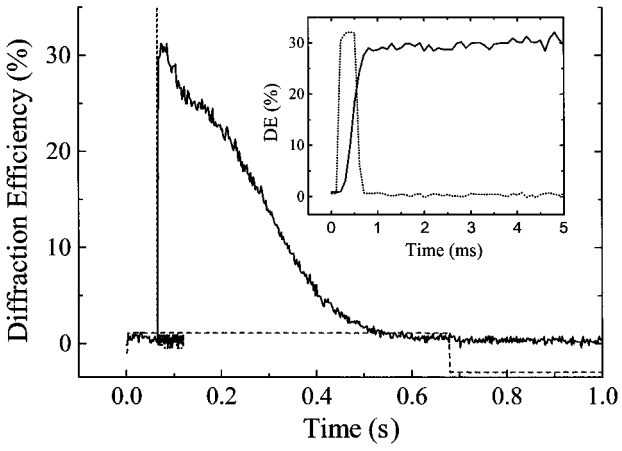

Fig. 5. Transient diffraction hologram dynamics showing a 600-μs holographic write time with a 30% DE. The inset graph shows similar data taken with a higher temporal resolution.

Ferroelectric LC molecules within the bright regions experience a significantly stronger electric field and therefore rotate quickly compared with those in the dark regions, creating a polarization-dependent index grating that has a period equal to that of the interference fringe spacing within the LC layer. Optimization of both the driving voltage and the write-light intensity causes those LC molecules in the bright areas to rotate quickly, whereas those in the dark regions maintain their orientation for an extended period, creating a persistent grating. Eventually, however, the dark-region molecules will rotate, and the grating will fade.

The experimental setup for characterizing this process is shown in Fig. 4. A 532-nm write beam is passed through an electronic LC shutter to control the temporal profile of the write pulse on the OASLM. The beam is then defocused and sent through a Mach–Zehnder-type interferometer such that the two write pulses interfere on the PC. This interference pattern creates the diffraction grating within the LC layer. The 810-nm read beam is diffracted by this grating, and the temporal dynamics of the first diffracted order are measured by a fast photodiode. Resolution measurements are made by variation of the angle between the two write beams. Because this prototypical device was not antireflection coated for 810 nm and there is some residual absorption in the PC at this wavelength, the DE is defined here as the power in the first diffracted order divided by the power of the transmitted beam when no grating is present. We define the holographic write time of the device as the time interval from the onset of the write pulse until the DE reaches 90% of its maximum value.

Figure 5 shows plots of the write pulse (dotted curve) and the voltage (dashed curve) adjusted to minimize the holographic write time but still maintain a relatively high DE. In this case the spatial frequency of the interference pattern is measured to be 18 lp/mm because of the ~0.5° angle between the write beams. Using a 0.4-ms (FWHM) write pulse with an energy of 400 nJ/cm^2 and setting the voltage pulse from −42.5 V to 16 V with a 1-s period yields a peak DE of 31% and a holographic write time of approximately 600 μs, as shown in the inset. Experimentally there is a trade-off between fast response and high DE. Although the rate of rotation of the index ellipsoid can be increased, eventually the DE declines with increasing applied voltages because the dark-region LC molecules are also rotating quickly. With slight adjustments to the write pulse and the voltage, a 34% DE can be achieved, but the holographic write time is approximately 5 ms. Experimentally the highest DE occurs when the OASLM is rotated such that the LC layers are perpendicular to the grating vector. Also, the DE is improved moderately by the alignment of the polarization of the read beam with the grating vector, an observation that currently is being investigated.

Figure 6 shows how the peak in the DE curve varies with the spatial frequency, which can be adjusted by changing the angle between the writing beams. For each spatial frequency the DE is maximized with small adjustments to both the voltage and the write pulses. At 370 lp/mm an 8% DE is still achieved.

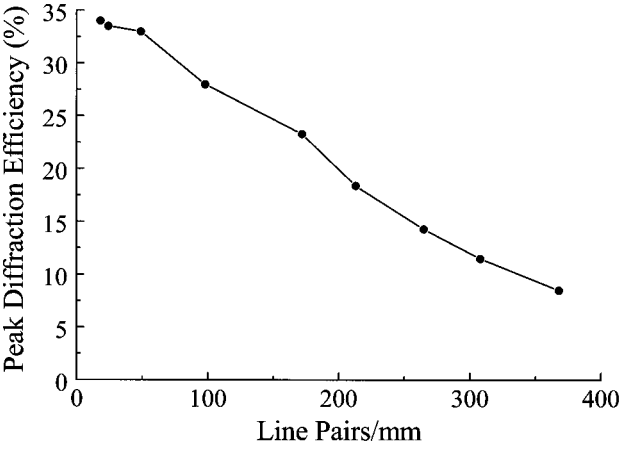

Fig. 6. Peak DE versus grating spatial frequency.

Note that, when the spatial frequency is less than 50 lp/mm, the grating spacing is measured directly by imaging the interference pattern onto a camera. Higher frequencies are inferred by measurement of the angle separating the zeroth and first diffracted orders.

Because the DE goes completely to zero (Fig. 5), we believe that all the LC molecules have been given enough time to rotate and that all remnants of the grating have been eliminated, as illustrated by the fade portion of Fig. 3. Therefore grating memory in the LC should not be an issue, despite the fact that an identical grating is being rewritten every cycle. To verify this, we adjusted the setup so that a spatially shifted diffraction grating was written on the PC every period. Affixing one of the mirrors in the interferometer to a piezoelectric transducer, as shown in Fig. 4, translates the interference pattern in time as the mirror oscillates. The dithering mirror is driven by a triangle-wave voltage whose amplitude is set such that the optical path length changes by exactly one wave (a 2π phase shift) at the peak voltage. This shift causes the fringe pattern on the OASLM to shift spatially one complete fringe before returning back to its original position. With the piezoelectric transducer dithering at 1.0 kHz and using the same voltage and write pulses as those used to generate the data taken with a stationary mirror (Fig. 5), the measured DE and holographic write time of the device are similar. There is, however, an approximately 5% reduction in the DE that is most likely due to the fact that the mirror is moving during the 0.1-ms pulse width of the write light. The grating therefore becomes slightly washed out. We believe that this reduction would be eliminated by use of shorter write pulses with the same pulse energy, but unfortunately our equipment was not able to deliver such pulses. It should be noted that care was taken to ensure that the write pulse and the mirror were not synchronous in such a way that the write pulse happened to strike the mirror when the mirror was in the same position during each cycle.

Depending on the application, the data-acquisition rate could be an important consideration for real-time holography. This refresh or frame rate is the time it takes to write, read, and then erase the grating. Figure 5 shows a 1-Hz refresh rate that is used so that the dark-region molecules have time to rotate completely and the DE goes to zero. If faster acquisition rates are required, the voltage could be switched, and an erase pulse could be introduced immediately after the grating is read to reinitialize all the molecules. Thus the refresh rate is limited by only the holographic write time of the device and the time needed to read the signal, which is determined by the application.

By significantly altering the amplitude and the period of the applied voltage, we can cause a high DE to last for an extended period of time. Figure 7 shows a 34% DE maintained for nearly 40 ms of the 48-ms period before the grating is erased. In this case a grating is established when the voltage switches from

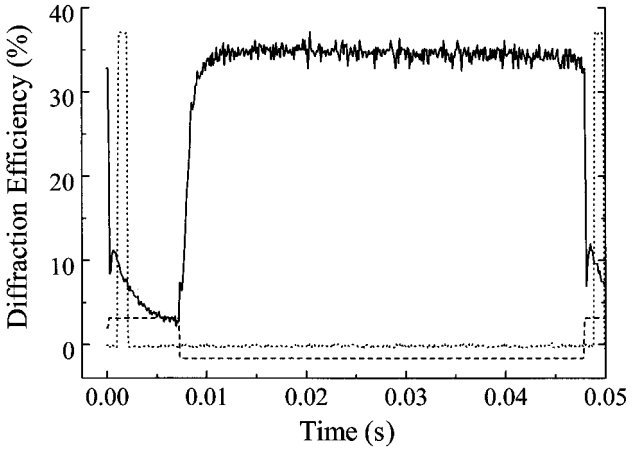

Fig. 7. Time-resolved DE showing high-duty-cycle operation.

+39 V to −21 V, even though write light is not present, because the carrier lifetime in the PC layer is much longer than the 48-ms period. Because the write pulse occurs during the initializing portion of the cycle (Fig. 3), the enhanced electric field across the LC in the bright regions simply increases the speed at which those molecules rotate back to the initial orientation. The molecules in the dark regions never rotate completely, and +39 V is high enough to cause them to reset quickly to the initial orientation. After the voltage switches to −21 V the carriers quickly migrate across the PC layer, increasing the local field across the LC layer. This sequence creates the spatially varying field across the LC layer that forms the grating. Figure 7 shows that the energy of each 1.0-ms-long write pulse is only 36 nJ/cm^2 and that the spatial frequency of the grating is 18 lp/mm. These results are promising for applications that require a high average signal because the DE can be maintained for 83% of the duty cycle. Here, however, the DE never reaches zero during the erase portion of the cycle, indicating that the grating never totally disappears. Such a situation might be useful only if the interference pattern, hence the diffraction grating, does not change significantly from period to period.

3. Conclusion

To apply RTH phase subtraction to dynamic aberration-compensation systems, it is necessary that spatial light modulators simultaneously fulfill demanding resolution, speed, efficiency, and sensitivity requirements. A novel OASLM that uses a DH-FLC and a carbon-doped a-Si:H photoconductor appears to be the first such device that is capable of simultaneously meeting all these requirements. Specifically, this device has demonstrated a 31% DE with a 600-μs holographic write time at a spatial frequency of 18 lp/mm with write-beam intensities of 400 nJ/cm^2. It is also capable of producing an 8% DE at a spatial frequency of 370 lp/mm. Such a device could be used to compensate severe aberrations that change on a millisecond time scale.

We gratefully acknowledge the contributions of Vladimir Venediktov, Alexey Leshchev, Leonid Soms, Donald Lubin, and Roger Ramsey.

References and Notes

1. N. L. Ivanova, A. P. Onokhov, A. N. Chaika, V. V. Resnichenko, D. N. Yeskov, A. L. Gromadin, N. A. Feoktistov, and L. A. Beresnev, "Liquid crystal spatial light modulators for adaptive optics and image processing," in *Advances in Optical Information Processing VII*, D. R. Pape, ed., Proc. SPIE **2754,** 180–185 (1996).
2. M. T. Gruneisen, K. W. Peters, and J. M. Wilkes, "Compensated imaging by real-time holography with optically addressed liquid-crystal spatial light modulators," in *Liquid Crystals*, I. Khoo, ed., Proc. SPIE **3143,** 171–181 (1997).
3. M. V. Vasil'ev, V. A. Berenberg, A. A. Leshchev, P. M. Semenov, and V. Yu. Venediktov, "Large numerical aperture imaging bypass system with dynamic holographic correction for primary mirror distortions," in *Adaptive Optical System Technologies*, D. Bonaccini and R. K. Tyson, eds., Proc. SPIE **3353,** 889–895 (1998).
4. An in-depth description of the LC molecular behavior can be found in *Spatial Light Modulator Technology: Materials, Devices, and Applications*, U. Efron, ed. (Marcel Dekker, New York, 1995).
5. J. W. Goodman, D. W. Jackson, M. Lehmann, and J. Knotts, "Experiments in long-distance holographic imagery," Appl. Opt. **8,** 1581–1586 (1969).
6. S. Fukushima and T. Kurokawa, "Real-time hologram construction and reconstruction using a high-resolution spatial light modulator," Appl. Phys. Lett. **58,** 787–789 (1991).
7. B. Landreth, C. C. Mao, and G. Moddel, "Operating characteristics of optically addressed spatial light modulators incorporating distorted helix ferroelectric liquid crystals," Jpn. J. Appl. Phys. **30,** 1400–1404 (1991).
8. G. B. Cohen, R. Pogreb, K. Vinokur, and D. Davidov, "Spatial light modulator based on a deformed-helix ferroelectric liquid crystal and a thin a-Si:H amorphous photoconductor," Appl. Opt. **36,** 455–459 (1997).
9. A. P. Onokhov, V. A. Berenberg, A. N. Chaika, N. L. Ivanova, M. V. Isaev, N. A. Feoktistov, L. A. Beresnev, and W. Haase, "Novel liquid-crystal spatial light modulators for adaptive optics and image processing," in *Advances in Optical Information Processing VIII*, D. R. Pape, ed., Proc. SPIE **3388,** 139–148 (1998).
10. Hamamatsu technical data sheets for the Model X5641 PAL-SLM parallel-aligned nematic LC spatial light modulator and the Model X4601 FLC-SLM ferroelectric LC spatial light modulator (Hamamatsu Corporation, 360 Foothill Road, Bridgewater, N.J. 08807, 1997).
11. C. C. Mao, K. M. Johnson, and G. Moddel, "Optical phase conjugation using optically addressed chiral smectic liquid crystal spatial light modulators," Ferroelectrics **114,** 45–53 (1991).
12. L. A. Beresnev, L. M. Blinov, and D. I. Dergachev, "Electrooptical response of a thin layer of a ferroelectric liquid crystal with a small pitch and high spontaneous polarization," Ferroelectrics **85,** 173–186 (1988).
13. K. Akiyama, A. Takimoto, and H. Ogawa, "Photoaddressed spatial light modulator using transmissive and highly photosensitive amorphous-silicon carbide film," Appl. Opt. **32,** 6493–6500 (1993).
14. Y. Hamakawa, ed., *Amorphous Semiconductor Technologies and Devices* (Ohmsha, Ltd., Tokyo, 1981).
15. L. A. Beresnev, W. Dultz, A. Onokhov, and W. Haase, "Local optical limiting devices based on photoaddressed spatial light modulators, using ferroelectric liquid crystals," Mol. Cryst. Liq. Cryst. **304,** 285–293 (1997).
16. I. Abdulhalim and G. Moddel, "Electrically and optically controlled light modulation and color switching using helix distortion of ferroelectric liquid crystals," Mol. Cryst. Liq. Cryst. **200,** 79–101 (1991).